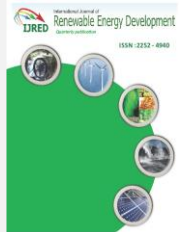




Contents list available at IJRED website

International Journal of Renewable Energy Development

Journal homepage: <https://ijred.undip.ac.id>



Research Article

Methods for Fault Location in High Voltage Power Transmission Lines: A Comparative Analysis

Truong Ngoc Hung*

Department of I.T., FPT University - Quy Nhon A.I Campus, Nhon Binh Ward, Quy Nhon City, Binh Dinh Province, Viet Nam

Abstract. Power transmission system stability can be significantly affected due to faults. The fault location accuracy in the transmission lines can make many benefits such as acceleration of the line restoration, reduction in cost, breakdown time, maintenance, and time searching. The methods based on the impedance, including the simple reactance, Takagi, modified Takagi, and double-end, are very much appreciated for locating the fault in transmission lines and especially by estimating the fault distance. This study proposes a comparative case study between these methods. The theoretical basis and the analysis, calculation, and estimation of each method are specifically re-established. To observe the performance of each method, a practical 220kV Quy Nhon - Tuy Hoa transmission line in Vietnam is used to simulate, calculate, evaluate, and compare under the various fault types and resistances. The power system is modeled and simulated in the MATLAB/Simulink software via the time domain. The voltage and current measurements at two ends of the line are used to determine the fault location on the Quy Nhon - Tuy Hoa transmission line. The simulation results show clearly the effectiveness of each fault location method.

Keywords: Fault location, Transmission line, Power system stability, Global positioning system, Grid faults



@ The author(s). Published by CBIORE. This is an open access article under the CC BY-SA license (<http://creativecommons.org/licenses/by-sa/4.0/>).

Received: 31st May 2022; Revised: 7th August 2022; Accepted: 15th August 2022; Available online: 22nd August 2022

1. Introduction

Electric transmission line plays a vital role in a power system to deliver electrical energy from generating sites, such as power substations or power plants, to electrical substations where voltage is transformed and distributed to consumers or other substations (Blume 2016; Daza 2016). It can be assumed that the electric transmission line is the backbones or the highways of the power system for moving electrical energy efficiency and safety over long distances. The faults in transmission lines due to some possible causes, including lightning, wind, apparatus failure, etc., are major causes of power outages. The fault location accuracy in the transmission lines can make many benefits such as acceleration of the line restoration, reduction in cost, breakdown time, maintenance, and time searching (Saha *et al.* 2009; Zimmerman *et al.* 2003).

In general, the overall process of automatically locating faults in electric transmission lines is described in Fig. 1 (Farhangi 2014). In which, the COMTRADE data, recorded by the relays when a short-circuit occurred on the transmission line (Phadke *et al.* 1992), is obtained at the centralized control system after the fault is tripped by the relays (Das *et al.* 2017; Gururajapathy *et al.* 2017). The signal processing methods depending on the selected fault location method are applied to obtain data, extract the significant features, and determine the fault location. In this stage, several signal processing methods, consisting of

the modal analysis and the wavelet transform, are used for the travelling wave-based method (Mosavi *et al.* 2016; Reis *et al.* 2021; Sawai *et al.* 2020; Fedorov *et al.* 2020), and the time domain and the frequency domain methods are applied to the impedance-based method (Han *et al.* 2020; Takagi *et al.* 1982; Namas and Džafić 2020; Barati and Doroudi 2018; Khoa and Tung 2018). The outputs of the signal process are considered as the inputs of the executed analytics to calculate the fault distance. The obtained results, including the fault type, location, duration, and current, etc., are stored in the database for further purposes like presentation, notification, and integration.

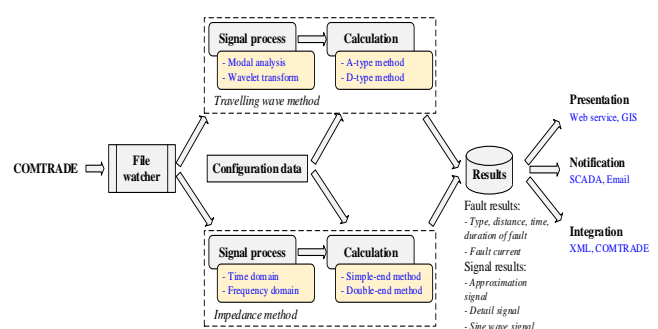


Fig. 1 Data flow and signal process of fault location algorithm.

* Corresponding author
Email: hungtn19@fe.edu.vn (T. N. Hung)

Recently, many approaches have been developed to locate the fault in electric transmission lines. The algorithm based on reactance measurements has been proposed to locate a fault on overhead lines of alternating current electrified railway (Han *et al.* 2020). A new fault locator was developed using the single-end measurements of voltage and current to determine the fault location (Takagi *et al.* 1982). The least-square method was applied in the method based on impedance to locate a fault in ungrounded networks (Namas and Džafić 2020). In Ref. (Barati and Doroudi 2018), the authors modified the impedance-based method for estimating the distance of fault in transmission lines in the presence of the fault current limiting. On the other hand, the travelling-based fault location methods have been proposed for estimating the fault location in the distribution network, such as the unsynchronized- and synchronized-based methods (Kalita *et al.* 2021; Chafi *et al.* 2021; Han *et al.* 2020), the adaptive convolution neural network-based method (Liang *et al.* 2020), and the single-end travelling wave fault location method (Xu *et al.* 2014).

The performance of the impedance-based fault location methods was comprehensively studied in Khoa, Cuong, Cuong and Hieu (2022). The single-ended fault location for hybrid distribution lines was based on the characteristic distribution of traveling wave along the line (Shu *et al.* 2003). The approach based on the ensemble Kalman filter was established to minimize outage time, labor, and costs of faults on transmission lines (Fan *et al.* 2018). The new technique for online tracking of fault location in distribution networks was introduced in Ahmed *et al.* (2021) to enhance system reliability and continuity of supply. Based on two-end measurements, Christos *et al.* (2022) proposed the two formulations of fault location algorithm which was appropriate for unbalanced medium voltage overhead distribution systems of radial network with or without distributed generations (Khoa, Van, Hung and Tuan, 2022; Saad *et al.* 2018). The fault location algorithm based on synchronous phasor measurement for shunt-compensated lines under dynamic conditions was proposed to overcome the uncertainties in the controller parameters of the shunt compensator device (Deng *et al.* 2022; Khoa *et al.* 2017). The novel fault location approach based on the exact distributed parameter line model and sparse estimation was proposed for transmission lines (Jia *et al.* 2022). The fault location method based on single-ended phasor measurements was developed from the real digital fault recorder (Felipe *et al.* 2022; Xie *et al.* 2022). The artificial intelligence (AI)-based fault location estimation method was developed for transmission lines only using the measurement from one end of the line (Swetapadma *et al.* 2021).

In general, all of the above-mentioned methods give good results for locating the fault in the transmission line, especially the impedance-based methods, in which the most significant is the simple reactance, the Takagi, modified Takagi, and double-end methods. In order to see the superiority of each method, this paper proposed a comparative case study to estimate the distance to fault in electric transmission lines. All related contents of these methods have been summarized and analyzed. A practical 220kV Quy Nhon - Tuy Hoa transmission line of Vietnam is used to simulate, calculate, evaluate, and compare under the fault conditions. In this paper, four types of fault, consisting of the single-phase to ground (SLG), phase-to-phase to ground (LLG), phase-to-phase (LL), and three-phase to ground (LLL) with the different fault resistance

are considered to occur at various locations in the electric transmission line corresponding to different operating modes. The Matlab/Simulink software is a tool to simulate.

The contributions of this paper are: (i) to establish the theoretical basis and the analysis, calculation, and estimation of four methods for locating faults in the high voltage transmission line based on the impedance between the sending and receiving ends, (ii) to analyze the accuracy of methods depending on the measured voltage and current signals, the fault resistance, and the fault location along the transmission line.

The remaining of this paper includes: Section 2 presents the background and methodology of the methods for locating the fault in the transmission lines. Section 3 demonstrates the simulation results and discussion for comparing the performance of the methods by simulation of the practical 220kV Vietnamese transmission line from the Quy Nhon (QN) substation to the Tuy Hoa (TH) substation. Finally, Section 4 concludes the paper.

2. Methods to locate the fault

Several methods to locate the fault in the transmission lines based on the impedance have been introduced to determine the fault distance in the transmission line. Each method has its peculiarities the require specific input data and make certain suppositions, which may or may not be true in a particular fault location situation. This study specifically re-establishes the theoretical basis and the analysis, calculation, and estimation of the simple reactance, Takagi, modified Takagi, and double-end methods based on the impedance. That is for comparative study of their performance.

The two-end transmission line is considered for the simulation modeling, as shown in Fig. 2, which is used to establish the fault location equations—assuming that a fault occurs on the transmission line at position F having a distance m per unit of the line length from the sending end and $(1-m)$ per unit of the line length from the receiving end. The impedance value of the line segment from the sending end to the fault position F is mZ_L and the impedance value of the line segment from the fault position F to the receiving is $(1-m)Z_L$. The fault resistance is R_F . The measured voltage and current of the sending and the receiving ends are V_S, I_S and V_R, I_R , respectively.

2.1. Single-end method

The single-end method uses a simple algorithm and for locating the fault in the transmission line with a standard for the numerical relays. For this method, the communication channels and remote data are not considered; The impedance value of the line segment seen by looking into the line from one end is calculated (Saha *et al.* 2009).

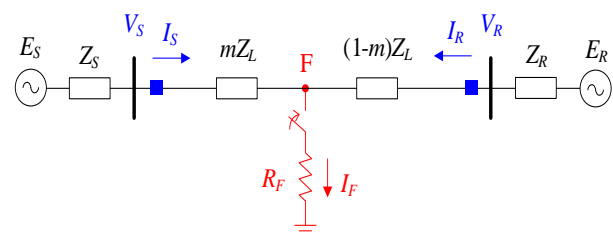


Fig. 2 Two-end transmission line.

Table 1
The measurements for different fault types.

| Fault type | V_S | I_S | ΔI_S |
|---------------|-------------|-----------------|---------------------------------------|
| AG | V_A | $I_A + kI_{S0}$ | $I_A - I_{Apre}$ |
| BG | V_B | $I_B + kI_{S0}$ | $I_B - I_{Bpre}$ |
| CG | V_C | $I_C + kI_{S0}$ | $I_C - I_{Cpre}$ |
| AB, ABG, ABCG | $V_A - V_B$ | $I_A - I_B$ | $(I_A - I_{Apre}) - (I_B - I_{Bpre})$ |
| BC, BCG, ABCG | $V_B - V_C$ | $I_B - I_C$ | $(I_B - I_{Bpre}) - (I_C - I_{Cpre})$ |
| CA, CAG, ABCG | $V_C - V_A$ | $I_C - I_A$ | $(I_C - I_{Cpre}) - (I_A - I_{Apre})$ |

where $k = Z_{L0}/Z_{L1} - 1$

The measures phase voltages and currents from the sending end are considered. Therefore, from Fig. 2, the sending end voltage is calculated as follows:

$$V_S = I_S (mZ_{L1}) + I_F R_F \tag{1}$$

where m is the fault distance, R_F is the fault resistance, I_F is the fault current, V_S and I_S are the sending end voltage and current, respectively depending on the fault type and are calculated as listed in Table 1. Whereas $V_A, V_B,$ and V_C are the A, B, and C phase voltages, respectively; $I_A, I_B,$ and I_C are the A, B, and C phase fault currents, respectively; $I_{Apre}, I_{Bpre},$ and I_{Cpre} are the A, B, and C phases pre-fault currents, respectively; Z_{L1} and Z_{L0} are the positive- and zero-sequence impedances of the transmission line, respectively.

The impedance from the sending end to the fault position is calculated as follows:

$$Z = \frac{V_S}{I_S} = mZ_{L1} + R_F \frac{I_F}{I_S} \tag{2}$$

As known, Eq. (2) is the condition to develop the single-end methods that are used to determine the distance to the fault, in which $m, R_F,$ and I_F are the variables to be determined. The impacts of R_F and I_F are eliminated on the accuracy of fault location results. Therefore, this method has been developed based on the line impedance and divided into three methods with the following procedures.

a) Simple reactance method

This method is developed based on the comparative of the line impedance of positive-sequence Z_{L1} and the impedance is calculated in Eq. (2) to determine the fault location. The accuracy of this method depends on the difference between the phase angle of I_S and I_F . If the R_F is ignored, the fault distance can be obtained as follows:

$$m = \frac{\text{Im}\left(\frac{V_S}{I_S}\right)}{\text{Im}(Z_{L1})} \tag{3}$$

where V_S and I_S are considered as listed in Table 1.

b) Takagi method

For this method, the fault distance can be obtained as follows

$$m = \frac{\text{Im}(V_S \times \Delta I_S^*)}{\text{Im}(Z_{L1} \times I_S \times \Delta I_S^*)} \tag{4}$$

where ΔI_S^* denotes the conjugate of ΔI_S is the deviation between the pre-fault and fault currents and can be considered as listed in Table 1.

Algorithm 1: Fault Identification Algorithm

```

Initialize The phase current phasors [ $I_A, I_B, I_C$ ]
The pick-up current setting  $I_{pickup}$ 
The initial fault type  $Type = "Normal"$ 
Calculate The zero-sequence current phasor  $I_0 = (I_A + I_B + I_C) / 3$ 
If ( $|I_A| \geq I_{pickup}$ ) & ( $|I_B| < I_{pickup}$ ) & ( $|I_C| < I_{pickup}$ ) & ( $|I_0| \geq I_{pickup}$ )
Then  $Type = "AG"$ 
If ( $|I_A| < I_{pickup}$ ) & ( $|I_B| \geq I_{pickup}$ ) & ( $|I_C| < I_{pickup}$ ) & ( $|I_0| \geq I_{pickup}$ )
Then  $Type = "BG"$ 
If ( $|I_A| < I_{pickup}$ ) & ( $|I_B| < I_{pickup}$ ) & ( $|I_C| \geq I_{pickup}$ ) & ( $|I_0| \geq I_{pickup}$ )
Then  $Type = "CG"$ 
If ( $|I_A| \geq I_{pickup}$ ) & ( $|I_B| \geq I_{pickup}$ ) & ( $|I_C| < I_{pickup}$ ) & ( $|I_0| \geq I_{pickup}$ )
Then  $Type = "ABG"$ 
If ( $|I_A| < I_{pickup}$ ) & ( $|I_B| \geq I_{pickup}$ ) & ( $|I_C| \geq I_{pickup}$ ) & ( $|I_0| \geq I_{pickup}$ )
Then  $Type = "BCG"$ 
If ( $|I_A| \geq I_{pickup}$ ) & ( $|I_B| < I_{pickup}$ ) & ( $|I_C| \geq I_{pickup}$ ) & ( $|I_0| \geq I_{pickup}$ )
Then  $Type = "CAG"$ 
If ( $|I_A| \geq I_{pickup}$ ) & ( $|I_B| \geq I_{pickup}$ ) & ( $|I_C| < I_{pickup}$ ) & ( $|I_0| < I_{pickup}$ )
Then  $Type = "AB"$ 
If ( $|I_A| < I_{pickup}$ ) & ( $|I_B| \geq I_{pickup}$ ) & ( $|I_C| \geq I_{pickup}$ ) & ( $|I_0| < I_{pickup}$ )
Then  $Type = "BC"$ 
If ( $|I_A| \geq I_{pickup}$ ) & ( $|I_B| < I_{pickup}$ ) & ( $|I_C| \geq I_{pickup}$ ) & ( $|I_0| < I_{pickup}$ )
Then  $Type = "CA"$ 
If ( $|I_A| \geq I_{pickup}$ ) & ( $|I_B| \geq I_{pickup}$ ) & ( $|I_C| \geq I_{pickup}$ ) & ( $|I_0| < I_{pickup}$ )
Then  $Type = "ABC"$ 
    
```

This method is improved compared to the simple reactance one by reducing the effect of load flow and minimizing the effect of fault resistance.

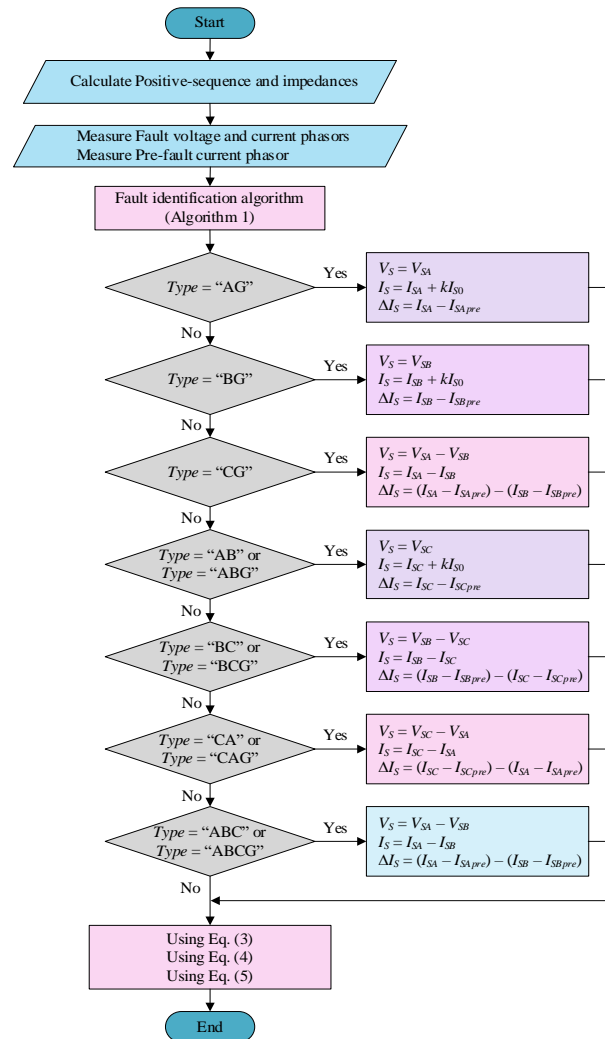


Fig. 3 The flowchart of the single-end methods

c) Modified Takagi method

The fault distance of this method can be obtained as follows

$$m = \frac{\text{Im}(V_s \times 3I_{s0}^*)}{\text{Im}(Z_{L1} \times I_s \times 3I_{s0}^*)} \tag{5}$$

where I_{s0} is the zero-sequence fault current measured at the sending end. This method was modified from the Takagi method by replacing the superposition current with the zero-sequence current of the sending end. This modification, it can limit ground faults since zero-sequence current exists for ground faults.

Therefore, the flowchart of the three above-mentioned methods shows in Fig. 3, and the fault identification is shown in Algorithm 1.

2.2. Double-end method

The fault distance of this method can be calculated as follows:

$$m = \frac{V_{S1} - V_{R1} + Z_{L1}I_{R1}}{(I_{S1} + I_{R1})Z_{L1}} \tag{6}$$

where V_{S1} and V_{R1} are the positive-sequence voltages of the sending and the receiving ends, respectively. I_{S1} and I_{R1} are the positive-sequence currents of the sending and the receiving ends, respectively.

For the three above-mentioned methods, it can conclude that the double-end method can be more accurate for locating the fault in the transmission line, but it requires data from both ends. The data must be captured from both ends before an algorithm can be applied. The double-end fault location algorithms calculate the fault location from the impedance seen from both ends of the line. Because of their accuracy in detecting fault location, these algorithms are usually better than one-end fault location algorithms.

3. Simulation Results and Discussion

3.1. Description of the test case

In this paper, to perform the comparative analysis of impedance-based methods for locating fault in power transmission lines, a practical Vietnamese electric transmission line (Khoa, Van, Hung and Tuan 2022) which is the 220kV overhead transmission line from the QN substation to the TH substation is modeled and simulated in the Matlab/Simulink software. The transmission line has the length $L = 92.5$ km with the positive-sequence line impedance $Z_{L1} = 38.471 \angle 80.31^\circ \Omega$, the zero-sequence line impedance $Z_{L0} = 129.204 \angle 81.10^\circ \Omega$. The transmission line is modeled as the distributed parameter model in the well-known Matlab/Simulink software (Gopalakrishnan *et al.* 2000). The two ends of the transmission line are connected to two grid sources which are represented as an ideal constant voltage source behind its inner equivalent impedance. For the tested system, both grid sources have the nominal frequency $f = 50$ Hz and the nominal voltage $V = 220$ kV. Whereas the QN sending source is represented by an ideal voltage source with $E_S = 1.0 \angle 10.0^\circ$ pu behind an equivalent positive- and zero-sequence impedance of $Z_{S1} = 3.75 \angle 71.0^\circ \Omega$ and $Z_{S0} = 11.25 \angle 65.0^\circ \Omega$, respectively.

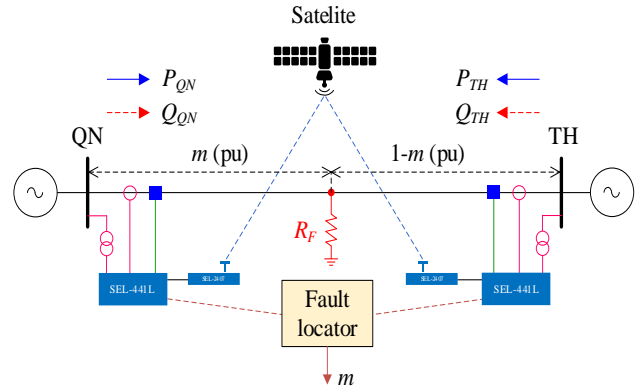


Fig. 4 The single-line diagram of the QN-TH 220kV transmission line of Vietnam.

Similarly, the TH receiving source is represented by an ideal voltage source with $E_R = 1.0 \angle 0.0^\circ$ pu behind an equivalent positive- and zero-sequence impedance of $Z_{R1} = 12.0 \angle 71.0^\circ \Omega$ and $Z_{R0} = 30.0 \angle 65.0^\circ \Omega$, respectively. In addition, the SEL-441L protection relays of the two ends receive the current and voltage signals from the current and voltage transformers, respectively to trip the fault current. Besides, the protection relays can communicate with the centralized control system via the private Wide Area Network (WAN) network or the Global Positioning System (GPS). The single-line diagram of the test system is shown in Fig. 4.

The fundamental components of voltage and current at the two ends of the transmission line are used to calculate the fault location. Thus, some filtering techniques should be applied to remove the DC offset and sub-harmonics in the voltage and current signals. Then, using the fast Fourier transform (FFT) is to determine the fundamental voltage and current (Han *et al.* 2020). Four types of fault consisting of SLG, LLG, LL, and LLLG faults are created at various locations on the transmission line to record the voltage and current signals at the two ends of the transmission line. In order to evaluate the accuracy of the impedance-based fault location methods, the location error is calculated the following terms:

$$Error(\%) = \frac{L_{calculated} - L_{actual}}{L} 100 \tag{7}$$

where L_{actual} is the actual length from the sending end to the fault location and $L_{calculated} = mL$ is the calculated length from the sending end to the fault location, in which L is the length of the line and m is the line length from the sending end to the fault location calculating per unit.

3.2. Simulation results

To estimate the distance to the fault in the electric transmission line, the impedance-based fault location methods are applied to calculate phasor quantities of voltage and current via the fast Fourier transform (FFT) (Das *et al.* 2017). However, when a fault occurs in a transmission line, there is an exponentially decaying DC offset in the fault current during the first few cycles as shown in Fig. 5, plotting the voltage and current waveforms of solid single-phase to ground fault on the line at the location of 0.6 pu far from the sending end. This DC offset will impact the estimation results of voltage and current phasor. To remove out the DC offset and extract

the voltage and current phasors, therefore, the FFT is applied with a one-cycle window length of the fundamental frequency and is performed repeatedly across the entire waveform (Fan *et al.* 2018).

From Fig. 5, when the phase A to ground fault occurred at 0.1 sec, the phase A current dramatically increases at that time, whereas the phase B and C currents are not varied during the fault. Besides, the three-phase voltages are almost unchanged during the fault excepting the voltage of the faulty phase is slightly decreased.

The fault voltage and current signals are recorded by the protection relays at two ends of the transmission line, and then they are transmitted to the centralized fault location system to estimate the distance to the fault. The phasors of the voltage and current are extracted by applying the FFT over one-cycle window length in the pre-fault and fault stages as shown in Fig. 5. These obtained phasor results are used to calculate the distance to fault based on the fault location methods. The current harmonic spectrum of the pre-fault and fault of phase A is shown in Fig. 6a and Fig. 6b, respectively. Observing Fig. 6a, the pre-fault current has no decaying DC offset with the total harmonic distortion $THD = 0.00\%$ and there are only the fundamental frequency currents of $I_A = 416.1\angle 21.1^\circ \text{ A}$, $I_B = 416.1\angle 261.1^\circ \text{ A}$, and $I_C = 416.1\angle 141.1^\circ \text{ A}$. These pre-fault currents represent the steady-state power flow of the transmission line.

When the fault occurs on phase A, the phase A current dramatically increases starting at the time of the fault and the decaying DC offset appears in the phase A current as shown in Fig. 6b. Applying the FFT over one-cycle window shown in Fig. 5, the THD of the phase A fault current is $THD = 1.8\%$ and the fundamental frequency currents of three phases are $I_A = 2941.0\angle -65.7^\circ \text{ A}$, $I_B = 297.2\angle 251.6^\circ \text{ A}$, and $I_C = 526.5\angle 132.2^\circ \text{ A}$.

For the test case in this paper, the practical Vietnam 220kV transmission line between the two QN and TH substations with 92.5 km in length is carried out to perform the comparative study to the above impedance-based fault location methods. The Matlab/Simulink software is used to make the simulation. It is supposed that a short-circuit occurs at various locations on the transmission line with the condition of m varied from 0.1 pu to 0.9 pu. The fault resistance depending on several specific fault conditions is unknown and uncertain. The fault location result of the impedance-based methods can also impact due to the fault resistance; therefore, this study investigates five fault resistances consisting of 0, 5, 10, 15, and 20 Ω at every fault location to simulate and evaluate the performance of the fault location methods. Fig. 7 shows the studied results of four methods for estimating the distance to fault for the SLG fault.

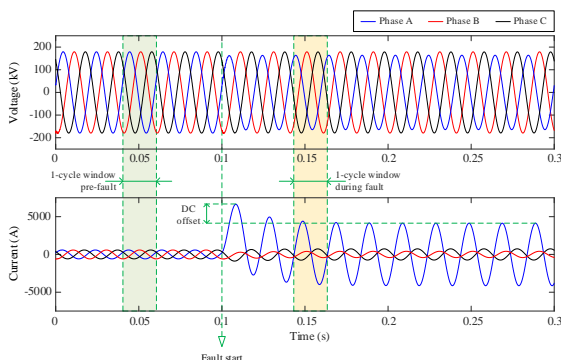


Fig. 5 The voltage and current waveforms at the sending end for the LG fault at $m = 0.6$ pu.

The location error defined in Eq. (7) is applied to show the effectiveness in Fig. 7. On the other hand, the location errors of the simple reactance method, the Takagi method, the modified Takagi method, and the double-end method are shown in Figs. 7 (a)-(d), respectively. It is clear that the location errors when using the simple reactance and the Takagi methods are higher than compared to the use of the modified Takagi and the double-end methods. Especially, the resistance value of fault is high, which will have more effects on the performance of the simple reactance and the Takagi methods. This problem is illustrated from the resistance and zero-sequence current values of fault in Eqs. (3) and (4), respectively. The modified Takagi and the double-end methods have small location errors as shown in Figs. 7(c) and (d), respectively. Their fault location results are not almost impacted by the fault resistance. This can ratiocinate from Eqs. (5) and (6). Observing Fig. 7, we can see that the double-end method has the smallest location error, which can be 0.00%. It can conclude that the fault resistance is not almost impacted. However, the errors are caused due to the shunt capacitance of the transmission line modeling.

In order to compare the performances of the methods based on the distance to fault, four locations corresponding to m values of 0.3, 0.5, 0.7, and 0.9 pu are carried to apply each method. The obtained results show in Fig. 8a-d, respectively. Observing Fig. 8, it is clear that the location errors are approximated zero to each method. However, the errors increase for the high resistance faults excepting the double-end method.

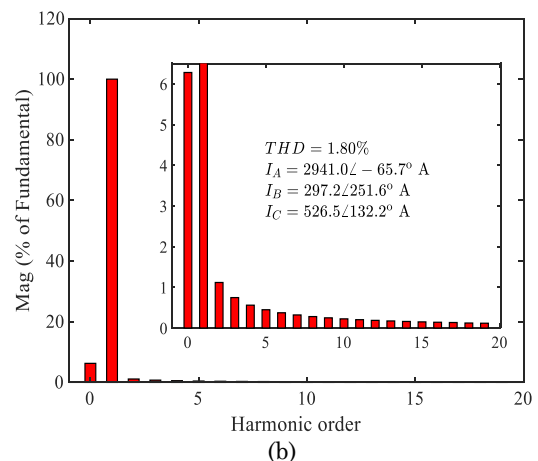
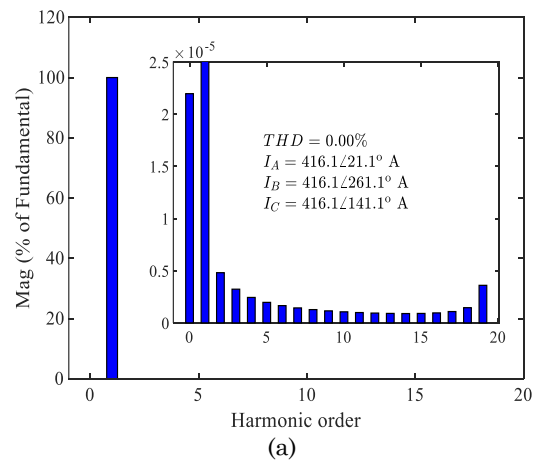


Fig. 6 The current harmonic spectrum of phase A: (a) the pre-fault and (b) the fault.

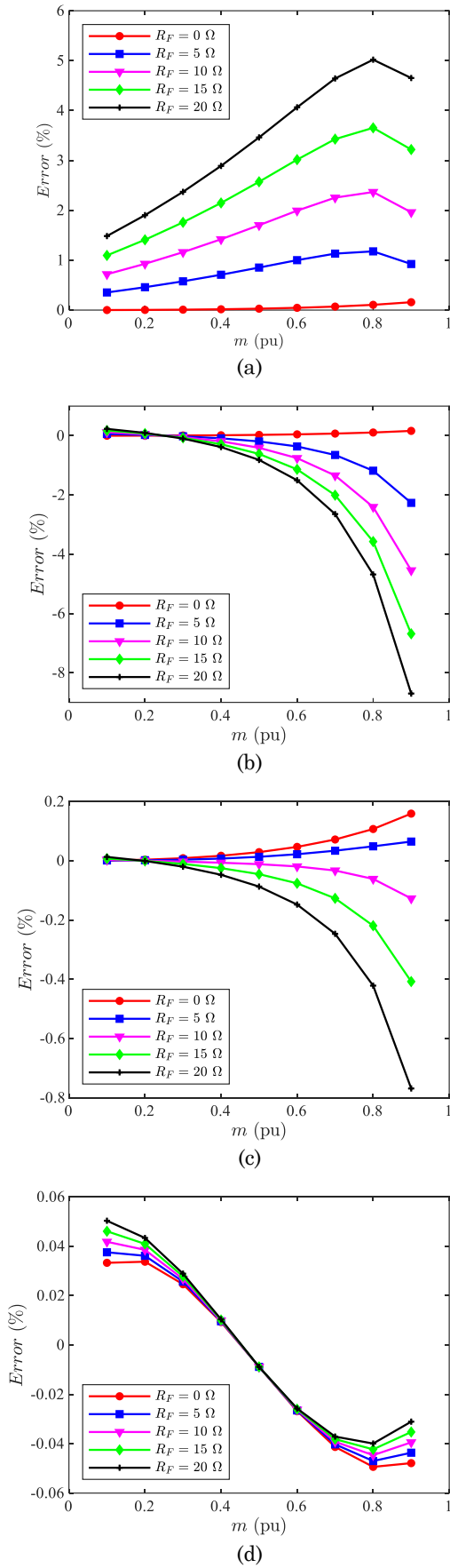


Fig. 7 The estimation result of the error between the methods: (a) Simple reactance method, (b) Takagi method, (c) Modified Takagi method, (d) Double-end method.

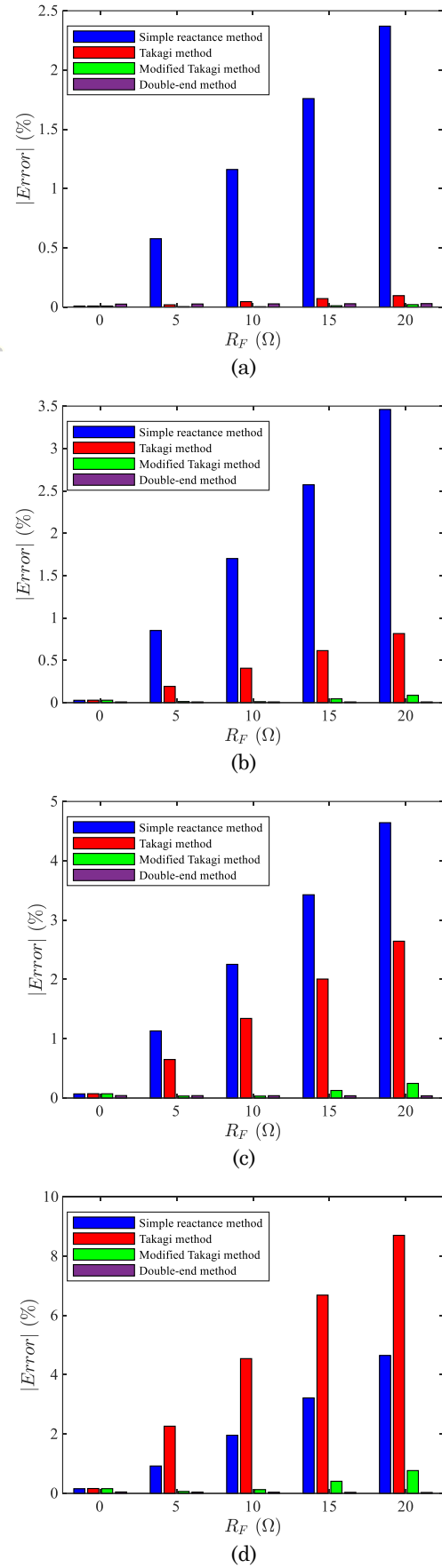


Fig. 8 The comparative results between the methods for different fault locations: (a) $m = 0.3$ pu, (b) $m = 0.5$ pu, (c) $m = 0.7$ pu, (d) $m = 0.9$ pu.

4. Conclusion

This paper performed a comparative study of the effectiveness of the impedance-based fault location methods used to estimate the distance to fault in electric transmission lines, including the simple reactance method, the Takagi method, the modified Takagi method, and the double-end method. All background and methodology of the methods were summarized and analyzed, and both their advantages and disadvantages were also discussed in this paper. The practical Vietnam 220kV overhead transmission line, having 92.5 kilometres long from the Quy Nhon substation to the Tuy Hoa substation, was modelled and simulated in the Matlab/Simulink software to verify the effectiveness of the fault location methods. We established four fault types consisting of the single-phase to ground (SLG), the phase-to-phase to ground (LLG), the phase-to-phase (LL), and the three-phase to ground (LLLG) faults with different fault resistances and locations along the line. The simulation results confirm that the accuracy of the methods only used voltage and current measurements of a single end depending on the fault resistance and location. Whereas the double-end method uses voltage and current measurements of two ends of the line to estimate the distance to fault, so its accuracy does not depend on the fault resistance and location. However, the double-end method needs good communication between two ends with the centralized control system via the private Wide Area Network (WAN) network or the Global Positioning System (GPS).

References

- Ahmed, N., ShetaGabr, M. A., Abdelfattah A. E. (2021). Online tracking of fault location in distribution systems based on PMUs data and iterative support detection. *International Journal of Electrical Power & Energy Systems*, 128, 106793; doi: [10.1016/j.ijepes.2021.106793](https://doi.org/10.1016/j.ijepes.2021.106793)
- Barati, J., Doroudi, A. (2018). Novel modified impedance-based methods for fault location in the presence of a fault current limiter. *Turkish Journal of Electrical Engineering & Computer Sciences*, 26(4), 1881-1893; doi: [10.3906/elk-1711-127](https://doi.org/10.3906/elk-1711-127)
- Blume, S. W. (2016). Electric power system basics for the nonelectrical professional. John Wiley & Sons
- Chafi, Z. S., Afrakhte, H. (2021). Wide area fault location on transmission systems using synchronized/unsynchronized voltage/current measurements. *Electric Power Systems Research*, 197, 107285; doi: [10.1016/j.epsr.2021.107285](https://doi.org/10.1016/j.epsr.2021.107285)
- Christos, A. A., Charalampos, G. A., Pavlos S. G., Vassilis C. N. (2022). Fault location algorithms for active distribution systems utilizing two-point synchronized or unsynchronized measurements. *Sustainable Energy, Grids and Networks*, 32, 100798; doi: [10.1016/j.segan.2022.100798](https://doi.org/10.1016/j.segan.2022.100798)
- Das, S., Santoso, S., Gaikwad, A., Patel, M. (2017). Impedance-based fault location in transmission networks: theory and application. *IEEE Access*, 2, 537-557; doi: [10.1109/ACCESS.2014.2323353](https://doi.org/10.1109/ACCESS.2014.2323353)
- Daza, S. A. (2016). Electric power system fundamentals. Artech House
- Deng, Y. J., Wang, C. M., Zhang, S., Han, W. Z. (2022). A fault location algorithm for shunt-compensated lines under dynamic conditions. *International Journal of Electrical Power & Energy Systems*, 143, 108387; doi: [10.1016/j.ijepes.2022.108387](https://doi.org/10.1016/j.ijepes.2022.108387)
- Fan, R., Liu, Y., Huang, R., Diao, R., Wang, S. (2018). Precise Fault Location on Transmission Lines Using Ensemble Kalman Filter. *IEEE Transactions on Power Delivery*, 33(6), 3252-3255; doi: [10.1109/TPWRD.2018.2849879](https://doi.org/10.1109/TPWRD.2018.2849879)
- Farhangi, H. (2014). IEEE guide for determining fault location on AC transmission and distribution lines. IEEE Stand. Assoc
- Fedorov, A., Petrov, V., Afanasieva, O., Zlobina, I. (2020). Limitations of traveling wave fault location. *2020 Ural Smart Energy Conference*, 21-25; doi: [10.1109/USEC50097.2020.9281153](https://doi.org/10.1109/USEC50097.2020.9281153)
- Felipe, V. L., et al. (2022). Single-ended multi-method phasor-based approach for optimized fault location on transmission lines. *Electric Power Systems Research*, 212, 108361; doi: [10.1016/j.epsr.2022.108361](https://doi.org/10.1016/j.epsr.2022.108361)
- Gopalakrishnan, A., Kezunovic, M., McKenna, S. M., Hamai, D. M. (2000). Fault location using the distributed parameter transmission line model. *IEEE Transactions on Power Delivery*, 15(4), 1169-1174; doi: [10.1109/61.891498](https://doi.org/10.1109/61.891498)
- Gururajapathy, S. S., Mokhlis, H., Ilias, H. A. (2017). Fault location and detection techniques in power distribution systems with distributed generation: A review. *Renewable and Sustainable Energy Reviews*, 74, 949-958; doi: [10.1016/j.rser.2017.03.021](https://doi.org/10.1016/j.rser.2017.03.021)
- Han, Z., Li, S., Liu, S., Gao, S. (2020). A reactance-based fault location method for overhead lines of AC electrified railway. *IEEE Transactions on Power Delivery*, 35(5), 2558-2560; doi: [10.1109/TPWRD.2020.2974162](https://doi.org/10.1109/TPWRD.2020.2974162)
- Jia, Y., Liu, Y., Wang, B., Lu, D., Lin, Y. (2022). Power Network Fault Location with Exact Distributed Parameter Line Model and Sparse Estimation. *Electric Power Systems Research*, In Press, 108137; doi: [10.1016/j.epsr.2022.108137](https://doi.org/10.1016/j.epsr.2022.108137)
- Kalita, K., Anand, S., Parida, S. K. (2021). A novel non-iterative fault location algorithm for transmission line with unsynchronized terminal. *IEEE Transactions on Power Delivery*, 36(3), 1917-1920; doi: [10.1109/TPWRD.2021.3054235](https://doi.org/10.1109/TPWRD.2021.3054235)
- Khoa, N. M., Tung, D. D. (2018). Locating fault on transmission line with static var compensator based on phasor measurement unit. *Energies*, 11(9), 2380; doi: [10.3390/en11092380](https://doi.org/10.3390/en11092380)
- Khoa, N. M., Cuong, M. V., Cuong, H. Q., Hieu, N. T. T. (2022). Performance Comparison of Impedance-Based Fault Location Methods for Transmission Line. *International Journal of Electrical and Electronic Engineering & Telecommunications*, 11(3), 234-241; doi: [10.18178/ijeetc.11.3.234-241](https://doi.org/10.18178/ijeetc.11.3.234-241)
- Khoa, N. M., Van, N. T. H., Hung, L. K., Tuan, D. A. (2022). Investigation of the Impact of Large-Scale Wind Power and Solar Power Plants on a Vietnamese Transmission Network. *International Journal of Renewable Energy Development*, 11(3), 863-870; doi: [10.14710/ijred.2022.43879](https://doi.org/10.14710/ijred.2022.43879)
- Khoa, N. M., Hieu, N. H., Viet, D. T. (2017). A study of SVC's impact simulation and analysis for distance protection relay on transmission lines. *International Journal of Electrical and Computer Engineering*, 7(4), 1686-1695; doi: [10.11591/ijece.v7i4.pp1686-1695](https://doi.org/10.11591/ijece.v7i4.pp1686-1695)
- Liang, J., Jing, T., Niu, H., Wang, J. (2020). Two-terminal fault location method of distribution network based on adaptive convolution neural network. *IEEE Access*, 8, 54035-54043; doi: [10.1109/ACCESS.2020.2980573](https://doi.org/10.1109/ACCESS.2020.2980573)
- Mosavi, M. R., Tabatabaei, A. (2016). Traveling-wave fault location techniques in power system based on wavelet analysis and neural network using GPS timing. *Wireless Personal Communications*, 86(2), 835-850; doi: [10.1007/s11277-015-2958-1](https://doi.org/10.1007/s11277-015-2958-1)
- Namas, T., Džafić, I. (2020). Least square method for impedance based fault location in ungrounded networks. *2020 2nd Global Power, Energy and Communication Conference*. 274-278; doi: [10.1109/GPECOM49333.2020.9247886](https://doi.org/10.1109/GPECOM49333.2020.9247886)
- Phadke, A. G. et al. (1992). Comtrade; a new standard for common format for transient data exchange. *IEEE Transactions on Power Delivery*, 7(4), 0885-8977; doi: <https://doi.org/10.1109/61.156995>
- Reis, R. L. A., Lopes, F. V., Neves, W. L. A., Fernandes Jr, D., Ribeiro, C. M. S., Cunha, G. A. (2021). An improved single-ended correlation-based fault location technique using traveling waves. *International Journal of Electrical Power & Energy Systems*, 132, 107167; doi: [10.1016/j.ijepes.2021.107167](https://doi.org/10.1016/j.ijepes.2021.107167)

- Saad, S. M., Nailly, N. E., Mohamed, F. A. (2018). Investigating the effect of DG infeed on the effective cover of distance protection scheme in mixed-MV distribution network. 7(3), 223-231; doi: [10.14710/ijred.7.3.223-231](https://doi.org/10.14710/ijred.7.3.223-231)
- Saha, M. M., Izykowski, J. J., Rosolowski, E. (2009). Fault location on power networks. Springer Science & Business Media.
- Sawai, S., Gore, R. N., Naidu, O. D. (2020). Novel traveling wave phase component-based fault location of transmission lines. 2020 IEEE International Conference on Power Electronics, Drives and Energy Systems, 1-5; doi: [10.1109/PEDES49360.2020.9379861](https://doi.org/10.1109/PEDES49360.2020.9379861)
- Shu, H., Liu, X., Tian, X. (2021). Single-Ended Fault Location for Hybrid Feeders Based on Characteristic Distribution of Traveling Wave Along a Line. IEEE Transactions on Power Delivery, 36(1), 339-350; doi: [10.1109/TPWRD.2020.2976691](https://doi.org/10.1109/TPWRD.2020.2976691)
- Swetapadma, A., Chakrabarti, S., Abdelaziz, A. Y., (2021). Feasibility study of intelligent fault location estimation methods for double-circuit transmission lines. International Transactions on Electrical Energy Systems, 31(12), e13198; doi: [10.1002/2050-7038.13198](https://doi.org/10.1002/2050-7038.13198)
- Takagi, T., Yamakoshi, Y., Yamaura, M., Kondow, R., Matsushima, T. (1982). Development of a new type fault locator using the one-terminal voltage and current data. IEEE Transactions on Power Apparatus and Systems, 8, 2892-2898; doi: [10.1109/TPAS.1982.317615](https://doi.org/10.1109/TPAS.1982.317615)
- Xu, F., Dong, X. (2014). A novel single-ended traveling wave fault location method based on reflected wave-head of adjacent bus. 12th IET International Conference on Developments in Power System Protection; doi: [10.1049/cp.2014.0048](https://doi.org/10.1049/cp.2014.0048)
- Zimmerman, K., Novosel, V. (2003). Draft guide for determining fault location on AC transmission and distribution lines, Piscataway, NJ USA
- Xie, J., Jin, G., Wang, Y., Nid, X., Liu, X. (2022). New Algorithm for 2-terminal Transmission Line Fault Location Integrating Voltage Phasor Feature and Phase Angle Jump Checking. Electric Power Systems Research, 209, 107971; doi: [10.1016/j.epsr.2022.107971](https://doi.org/10.1016/j.epsr.2022.107971)



© 2022. The Author(s). This article is an open access article distributed under the terms and conditions of the Creative Commons Attribution-ShareAlike 4.0 (CC BY-SA) International License (<http://creativecommons.org/licenses/by-sa/4.0/>)